Investigation of Efflorescence of Inorganic Aerosols Using Fluorescence Spectroscopy

Man Yee Choi and Chak K. Chan*

Department of Chemical Engineering, Hong Kong University of Science and Technology, Clear Water Bay, Kowloon, Hong Kong, China

Received: May 3, 2004; In Final Form: September 27, 2004

The phase transition is one of the most fundamental phenomena affecting the physical and chemical properties of atmospheric aerosols. Efflorescence, in particular, is not well understood, partly because the molecular interactions between the solute and water molecules of saturated or supersaturated solution droplets have not been well characterized. Recently, we developed a technique that combines the use of an electrodynamic balance and a fluorescence dye, 8-hydroxyl-1,3,6-pyrenetrisulfonate (pyranine), to study the distributions of solvated and free water in aqueous droplets (Choi, M. Y.; Chan, C. K.; Zhang, Y. H. *J. Phys. Chem. A* **2004**, *108,* 1133). We found that the equality of the amounts of solvated and free water is a necessary but not sufficient condition for efflorescence. For efflorescing compounds such as Na_2SO_4, $(NH_4)_2SO_4$, and a mixture of NaCl and Na_2SO_4, the amount of free water decreases, while that of solvated water is roughly constant in bulk measurements and decreases less dramatically than that of free water in single-particle measurements as the relative humidity (RH) decreases. Efflorescence of the supersaturated droplets of these solutions occurs when the amounts of free and solvated water are equal, which is consistent with our previous observation for NaCl. For noneffloresing compounds in single-particle levitation experiments such as $MgSO_4$ and $Mg(NO_3)_2$, the amounts of free and solvated water are equal at a water-to-solute molar ratio of about 6, at which spectral changes due to the formation of contact ion pairs between magnesium and the anions occur as shown by Raman spectroscopy. Fluorescence imaging shows that the droplets of diluted $Mg(NO_3)_2$ (at 80% RH) and $MgSO_4$ are homogeneous but those of NaCl, Na_2SO_4, $(NH_4)_2SO_4$, and supersaturated $Mg(NO_3)_2$ (at 10% RH) are heterogeneous in terms of the solvated-to-free water distribution. The solvated-to-free water ratios in NaCl, Na_2SO_4, and $(NH_4)_2SO_4$ droplets are higher in the outer regions by about half a radius deep than at the center of the droplets.

Introduction

The ability of atmospheric aerosols to absorb or evaporate water has profound influence on their physical and chemical properties and on their environmental impacts including global climate change. Phase transitions can induce dramatic changes in the size and composition of atmospheric aerosols. However, these processes, especially efflorescence, are not fully understood.[2−5] Many species, such as NaCl and $(NH_4)_2SO_4$, effloresce at low relative humidity (RH), but some others, such as NH_4NO_3 (ref 2), $Mg(NO_3)_2$, and $MgSO_4$, do not effloresce in single-particle experiments.[6] These particles retain water at RH below 10%.

Most studies on efflorescence provide information on the efflorescence relative humidity (ERH) and the concentration of the aerosol when efflorescence takes place. While the reported measurements in the literature are in general consistent, the process of efflorescence is poorly understood in terms of the ability to predict when efflorescence of supersaturated droplets takes place. Because an aqueous aerosol droplet is saturated or even supersaturated when it effloresces, the molecular interaction between the solvated water and the solute is expected to be very strong.[7] Information on the state of water as a droplet becomes supersaturated and finally effloresces helps us understand the hygroscopic properties and efflorescence of atmospheric aerosols.

Recently, we developed a single-particle fluorescence spectroscopic technique to investigate the state of water (solvated water vs free water) in aqueous droplets.[1] This technique involves the use of a dye that is sensitive to the proton-transfer ability in its environment and can be, in principle, applied to a wide range of aqueous solutions of chemical systems with pH higher than 3 (ref 8). Solvated water and free water refer, respectively, to the water molecules that interact directly with ions and to those in the bulk water phase that interact with other water molecules. In highly concentrated droplets, there are relatively stronger interactions between the solute and the solvated water molecules than between the solute and the free water molecules. Hence, the fluorescence responses of a diluted droplet and a concentrated (or supersaturated) one are very different. For instance, Chakraborty and Berglund[8] found that the condition of more free water than solvated water is required for maintaining a stable solvation structure in sugar solutions. The state of water as a function of the molar water-to-solute ratio (WSR), which is the sum of the ratios, of NaCl is shown in Figure 1. The amount of free water is always larger than that of solvated water, and the amounts of free and solvated water decreases as WSR decreases. Finally, efflorescence occurs at the corresponding ERH (WSR = 0.42, ref 9) when the amounts of solvated and free water are equal.

In this paper, we apply the single-particle fluorescence technique to investigate the solvated and free water distributions in some other inorganic aerosols that are known to effloresce. They are Na_2SO_4, $(NH_4)_2SO_4$, and a mixture of NaCl and Na_2SO_4. We confirm that the amount of free water is always larger

* Corresponding author. Tel.: (852) 2358-7124. Fax: (852) 2358-0054. E-mail: keckchan@ust.hk.

10.1021/jp048103h CCC: $30.25
Published on Web 01/26/2005

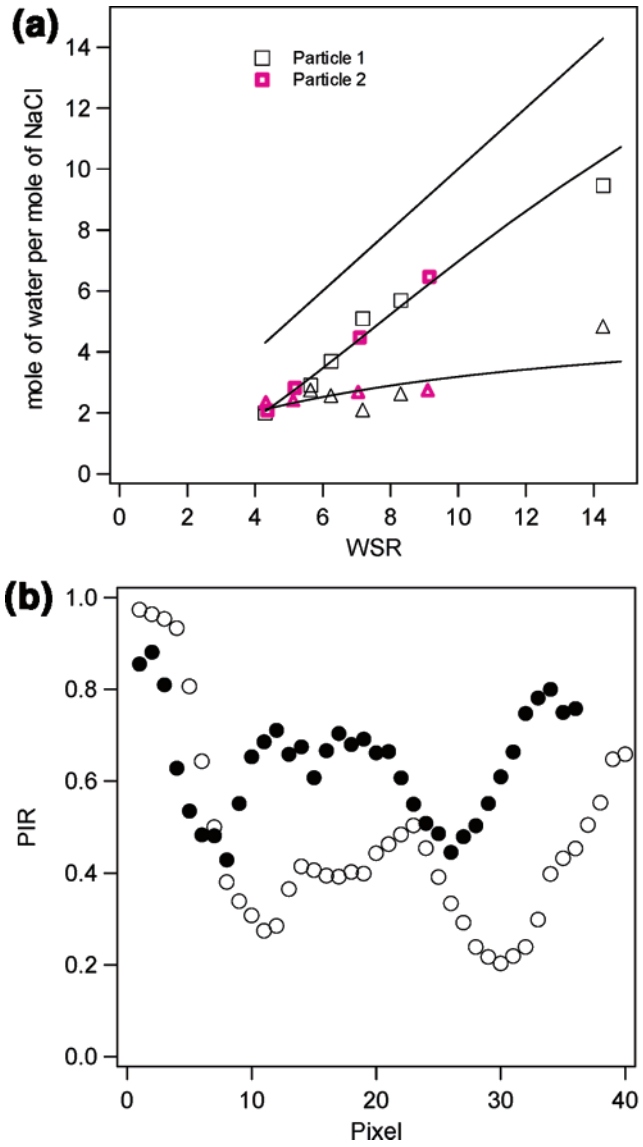

Figure 1. (a) Amounts of total, free, and solvated water per mole of sodium chloride as a function of WSR from single-particle studies (ref 1). −, total water; □, free water; △, solvated water. (b) The PIR of a NaCl droplet along the equator of the droplet. ○, PIR at RH = 80%; ●, PIR at RH = 70% (ref 1).

than or equal to the amount of solvated water in droplets of these solutions. The difference in the amounts of free water and solvated water becomes smaller as efflorescence is approached. At efflorescence, the amount of free water equals the amount of solvated water. In addition, we examine the solvated and free water distributions in $MgSO_4$ and $Mg(NO_3)_2$, which do not effloresce. We studied these two compounds because their hygroscopicities and their associations with their molecular structures have been characterized by Raman spectroscopy.[10−12] The results are discussed in terms of the molecular structures of the solutions of these aerosols at high supersaturation. Finally, we present our fluorescence imaging results to illustrate the spatial heterogeneity in terms of the solvated-to-free water ratio in droplets of selected compounds.

Method

The principle of the electrodynamic balance (EDB) has been well documented[13] and therefore is not described in detail here. The EDB is a unique device for studying supersaturated solutions because the particles are not in contact with any foreign surface and thus heterogeneous nucleation of solutions is suppressed. In a combination of AC and DC fields, a single charged particle of about 20 μm in diameter is trapped. The electrostatic force acting on the particle imposed by the DC voltage balances the weight of the particle and keeps the particle at the center of the balance. Hence, the mass of the particle equilibrated at different RH is proportional to the DC balancing voltage. The WSR of the particle can be calculated from the DC voltage. The Kelvin effect for the correction of vapor pressure due to curvature of the droplet is negligible for these large particles.

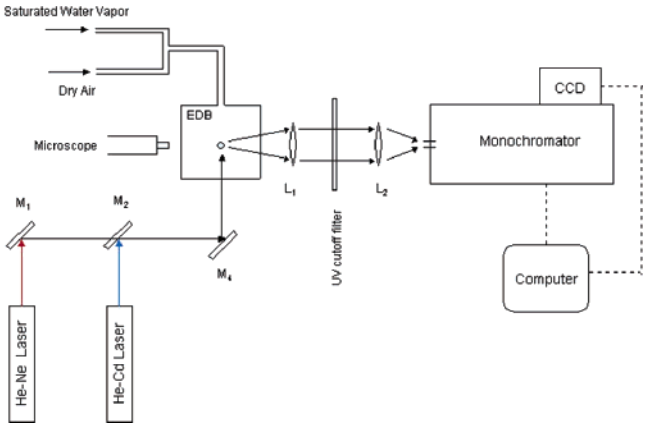

Figure 2. Schematic diagram of the experimental setup. M and L represent the mirror and the lens, respectively.

A single-particle fluorescence spectroscopy system consisting of an He−Cd laser (Kimmon IK3151R-E, CW = 325 nm, maximum power = 200 mW) and a 0.5 m monochromator (Acton SpectraPro 500) attached with a CCD (Andor Technology DV420-OE) was integrated with the EDB system, as shown in Figure 2. The 90° scattering of the levitated droplets in the EDB was focused onto the slit of the monochromator, after rejecting the Rayleigh scattering by a 320 nm UV cutoff filter. A 150 g/mm grating and an integration time of 20 s were selected in these measurements as well as in imaging experiments, which were made at ambient temperatures of 22−24 °C. In each individual measurement, the temperature varied less than 0.5 °C. The bulk measurements were obtained by using an optical fiber that was directly coupled to the slit of the monochromator. In each set of measurements, two to three particles were used and the results from these particles were consistent. Details of the experimental system and the experimental technique are described by Choi et al.[1]

Upon UV excitation, pyranine fluoresces and emits a broad spectrum, which generally consists of two broad peaks, one at around 440 nm (corresponding to the absence of free water or the presence of solvated water) and the other at around 510 nm (corresponding to the presence of free water). The peak intensity ratio (PIR) of the 440 nm peak to the 510 nm peak (PIR = I_{440}/I_{510}) in the fluorescence spectra is thus an indicator of the amount of solvated water to free water. The use of the peak intensity ratio method eliminates the effects of certain measurement variables such as laser intensity, collection optics, and the pyranine concentration. In our study, stock solutions of 100 ppm (1.9×10^{-4} M) of pyranine were prepared using 18 MΩ reverse osmosis water and pyranine (98% purity, Acros Organics) without further purification. The dye has been found to have negligible effects on the hygroscopicity, the occurrence of efflorescence, and the ERH of the compounds studied. For ammonium sulfate, the initial (at high RH) molar dye-to-water ratio was 3.43×10^{-6}, and the final (before ERH) molar dye-

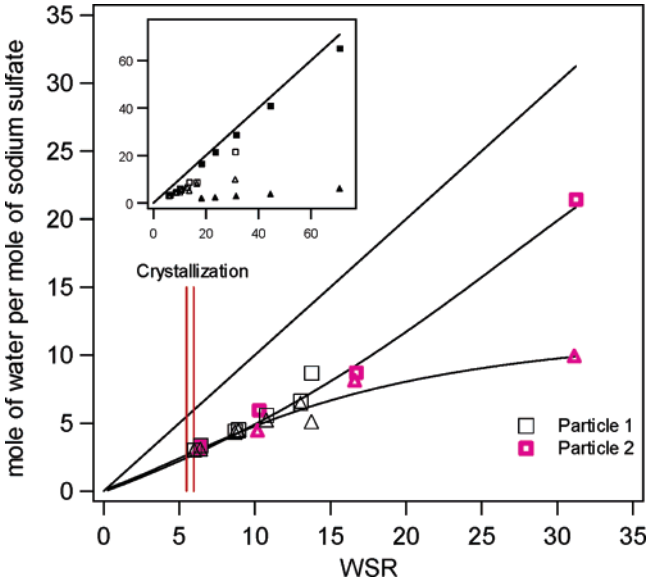

Figure 3. Amounts of total, free, and solvated water per mole of sodium sulfate as a function of WSR. −, total water in both single-particle and bulk measurements; □, free water in single-particle measurements; ■, free water in bulk measurements; △, solvated water in single-particle measurements; ▲, solvated water in bulk measurements. The vertical lines represent the range of ERH (ref 18).

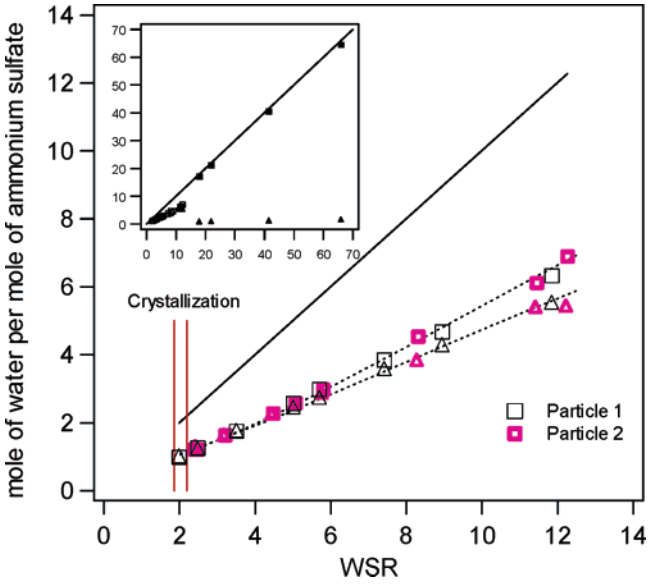

Figure 4. Amounts of total, free, and solvated water per mole of ammonium sulfate as a function of WSR. −, total water in both single-particle and bulk measurements; □, free water in single-particle measurements; ■, free water in bulk measurements; △, solvated water in single-particle measurements; ▲, solvated water in bulk measurements. The vertical lines represent the range of ERH (ref 19).

to-water ratio was 2.55×10^{-5}. The molar dye-to-solute ratio is constant at 6.15×10^{-5}. For $MgSO_4$, the final (at 20% RH) molar dye-to-water ratio $= 1.75 \times 10^{-5}$. Hence, even at supersaturation, the relative concentration of pyranine was low in the droplets. In fact, pyranine has been used to study the change in the water content during sol−gel processes.[14] Pyranine has also been used to measure the pH in the yeast *Yarrowia lipolytica* and in AOT reverse micelles (sodium bis(2-ethylhexyl) sulfosuccinate).[15,16] At pH greater than 3, pyranine's response depends solely on the state of water in its microenvironment.[17]

From the equilibrium hygroscopic measurements, we obtained the mass fraction of solute (mfs) of the droplet as a function of RH, which was then used to calculate the amount of total water per solute in the droplet. The overall experimental error in the hygroscopic measurements is within ±0.01 mfs for droplets, and the error in the determination of RH is estimated to be ±1% at RH = 40−80%. With sucrose (Choi et al., 2004), for which there are bulk pyranine measurements in the literature for comparison (Yuder and Berglund, 1996), as an example, the error in the ratio of free water to solute due to the error in mfs and RH is 4% and 2%, respectively, if the PIR is exact. The uncertainty in the determination of PIR from repeated measurements at a specific concentration is about 3%, which results in an overall error of about 2−4% in the ratios of free and solvated water to solute. Figure 1 illustrates the reproducibility of the ratios in the measurements using two particles. In the imaging experiments, the error in the PIR within a particle at a specific RH is about 10%. The larger error in the PIR from the imaging experiments is from the lower signal-to-noise ratios than in the fluorescence measurements.

Results and Discussion

(a) Efflorescence: Na_2SO_4, $(NH_4)_2SO_4$, and a Mixture of NaCl and Na_2SO_4. Figures 3−5 show the molar ratios of the free water to solute and the solvated water to solute as functions of the total water-to-solute ratio (i.e., WSR) of Na_2SO_4, $(NH_4)_2SO_4$, and a mixture of NaCl and Na_2SO_4 droplets in 1:1 mole ratio. The WSR, the sum of the free water-to-solute ratio and

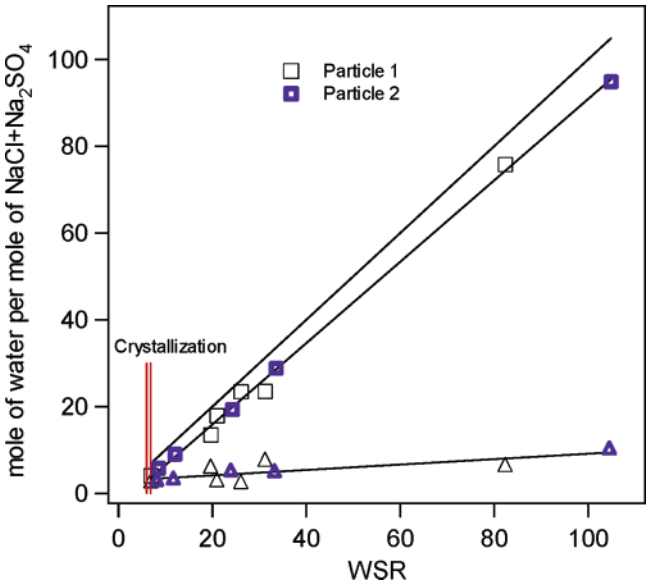

Figure 5. Amounts of total, free, and solvated water per mole of sodium chloride + sodium sulfate as a function of WSR. −, total water in both single-particle and bulk measurements; □, free water in single-particle measurements; △, solvated water in single-particle measurements. The vertical lines represent the range of ERH.

the solvated water-to-solute ratio, was determined from the hygroscopic measurements. In these figures, the bulk measurements (shown in the insets of Figures 3 and 4) and the single-particle measurements are indicated by solid and open symbols, respectively. When the WSR decreases as a result of the reduction of RH, the free water-to-solute ratio decreases. The solvated water-to-solute ratio decreases at a lower rate or remains relatively constant in the case of the $NaCl/Na_2SO_4$ mixture. Although the solvated water-to-solute and free water-to-solute ratios of $(NH_4)_2SO_4$ and Na_sSO_4 approach each other at low WSR, the former is always smaller than or equal to the latter.

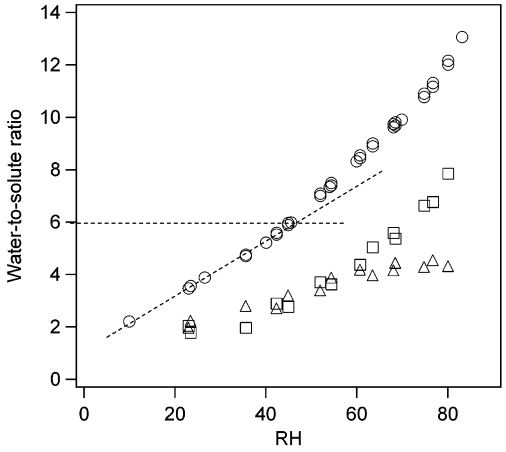

Figure 6. Hygroscopic data of magnesium sulfate droplets. ○, total water in single-particle measurements; □, free water in single-particle measurements; △, solvated water in single-particle measurements.

These particles remain as droplets until efflorescence takes place. The vertical lines represent the range of the measured ERH. The ERH values for Na_2SO_4, $(NH_4)_2SO_4$, and the NaCl/Na_2SO_4 mixture are 57−59% (ref 18), 37−40% (ref 19), and 32−37%, respectively. These values confirm that a trace amount of pyranine does not affect the ERH of these droplets. As we reported for NaCl (ref 1), the amounts of total water and free water are equal when the particles effloresce, although the amounts of free water and solvated water are very close to each other as they approach efflorescence in Na_2SO_4 and $(NH_4)_2SO_4$ droplets. It is believed that the condition of a larger amount of free water than solvated water is necessary to maintain a stable solvation structure.[8] In species that effloresce, when such conditions cannot be satisfied, the droplets effloresce to form solid particles. As will be shown next, equality of free water and solvated water was achieved in $MgSO_4$ and $Mg(NO_3)_2$ droplets but they did not effloresce. Hence, the equality of free water and solvated water is a necessary but not sufficient condition for efflorescence. In Figures 3 and 4, the bulk and single-particle measurements are not consistent. The single-particle measurements show a smaller amount of free water than the bulk measurements do at the same WSR. A similar discrepancy has been observed for NaCl droplets.[1] We discuss these discrepancies in section (c).

(b) No Efflorescence: $MgSO_4$ and $Mg(NO_3)_2$. Unlike typical inorganic salts such as NaCl, both $MgSO_4$ and $Mg(NO_3)_2$ do not effloresce at low RH in single-particle levitation experiments.[6] Figure 6 shows the equilibrium hygroscopic data for $MgSO_4$ in terms of WSR as a function of the percentage RH, which is equivalent to the water activity of the droplet multiplied by 100 at equilibrium. The WSR decreases nonlinearly with decreasing RH at high RH. However, a transition point at a WSR of about 6, below which the WSR decreases linearly with RH, is clearly observed. The WSR approaches unity as RH is extrapolated to zero. Zhang and Chan[10] observed a WSR of 1.5 at RH = 8%, which is consistent with the current measurements. The solvated water-to-solute ratio and the free water-to-solute ratio as a function of RH are also presented. They begin to merge at about 60% RH.

Shown in Figure 7 are the free water-to-solute and the solvated water-to-solute ratios as a function of the WSR of both bulk and single-particle measurements for $MgSO_4$, shown as filled and empty symbols, respectively. The bulk data are consistent with the single-particle data. The free water-to-solute ratio decreases linearly with decreasing WSR in the subsaturation region (WSR > 12), but it decreases less quickly in correlation with the WSR in the supersaturated region. The solvated water-to-solute ratio is more or less constant at around 4 when the WSR is larger than 8. Below a WSR of 8, the solvated water-to-solute ratio decreases gradually from 4 to 2 at 5% RH. In the literature, the solvation number of Mg^{2+} has typically been reported to be 6 (e.g., ref 20). The observation of a solvation number of 4 may be due to the strong tendency of magnesium ions to form contact ion pairs with sulfate ions, even in diluted solutions. Recently, Rudolph et al.[21] found that contact ion pairs can form in diluted $MgSO_4$ solutions, even at concentrations as low as 0.25 mol/L (WSR = 33.2).

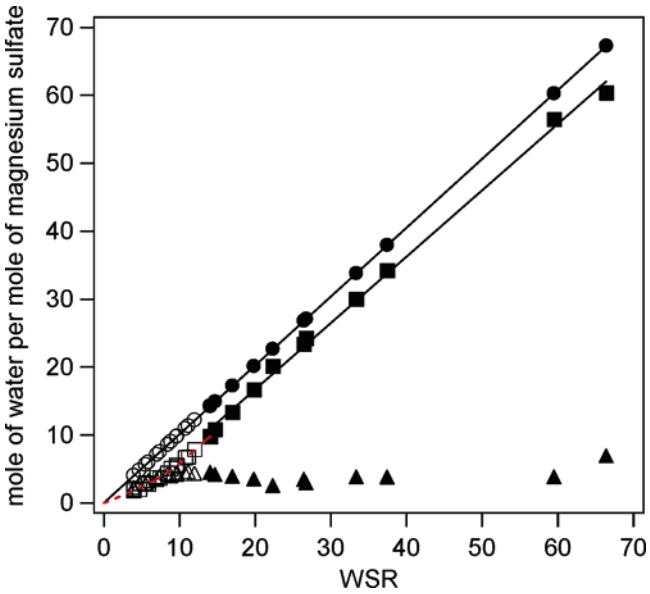

Figure 7. Amounts of total, free, and solvated water per mole of magnesium sulfate as a function of WSR from bulk and single-particle studies. ●, total water in bulk measurements; ○, total water in single-particle measurements; ■, free water in bulk measurements; □, free water in single-particle measurements; ▲, solvated water in bulk measurements; △, solvated water in single-particle measurements. The solid lines represent linear equation fitting, and the dotted curve represents quadratic equation fitting. There are three sets of single-particle data shown in the figure.

According to Figures 6 and 7, the amounts of free and solvated water are equal when the WSR is about 6.6 in $MgSO_4$ droplets. Although efflorescence does not take place, the equal amounts of the free water and solvated water indicate that there are possibly structural changes in the droplets at a WSR of around 6. Chan et al.[22] and Choi and Chan[23] observed that there is a significant retardation in the evaporation rate of mixed Na_2SO_4 and $MgSO_4$ droplets and in the growth rate of $MgSO_4$ droplets at a WSR of 6.6, which is close to the transition point in the equilibrium hygroscopic data at a WSR of 6 as shown in Figure 6.

These special observations of water sorption characteristics are consistent with the finding in this study of equal amounts of free and solvated water in $MgSO_4$ and the significant spectral changes in $MgSO_4$ droplets (the peak location and the full width at half-height of the Raman sulfate peak at about 980 cm^{-1}) observed by Zhang and Chan.[10] All of these events occur at a WSR of about 6, which is the hydration number of Mg^{2+} ions. Zhang and Chan[10] explained these Raman changes as coming from the formation of monodentate and bidentate contact ion pairs. In highly concentrated droplets, there are insufficient water molecules to complete the primary shell of hydration of the ions. Direct contact ion pairs between the cations and anions are expected to be abundant. The special observations of the

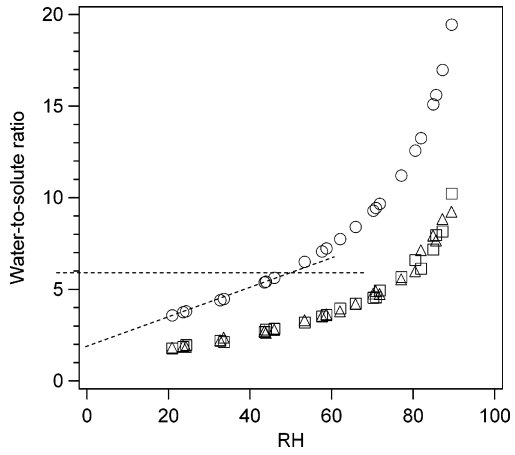

Figure 8. Hygroscopic data of magnesium nitrate droplets. ○, total water in single-particle measurements; □, free water in single-particle measurements; △, solvated water in single-particle measurements.

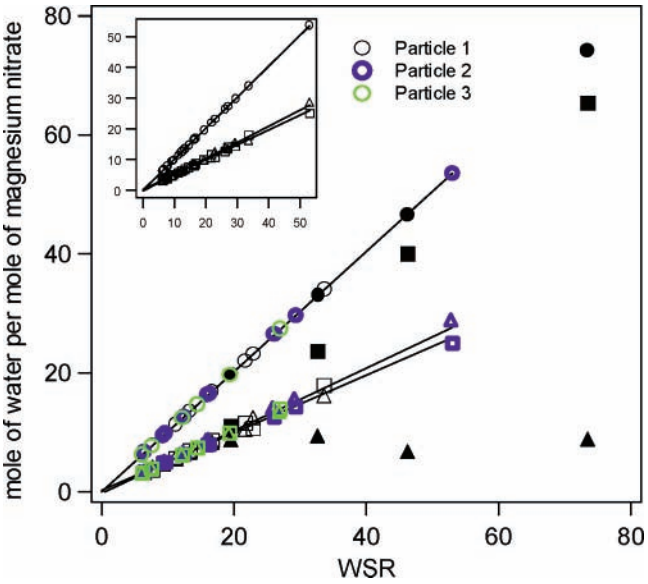

Figure 9. Amounts of total, free, and solvated water per mole of magnesium nitrate as a function of WSR from bulk and single-particle studies. ●, total water in bulk measurements; ○, total water in single-particle measurements; ■, free water in bulk measurements; □, free water in single-particle measurements; ▲, solvated water in bulk measurements; △, solvated water in single-particle measurements. The solid lines represent linear equation fitting.

fluorescence, hygroscopic, and Raman measurements at a WSR of 6 are related to the formation of a contact ion pair network containing direct ion contact pairs of Mg^{2+} and SO_4^{2-}. This study shows that the amount of solvated water per solute equals 3 at a WSR of 6. The hexa-coordination of Mg^{2+} is maintained by the direct contact ion pairs with sulfate and the solvated water.

Similar to $MgSO_4$, $Mg(NO_3)_2$ droplets do not effloresce in single-particle levitation experiments (Figures 8 and 9). A transition point at a WSR of 6 was also observed. The WSR approaches 2 when the RH is extrapolated to zero. Figure 9 shows the solvated water-to-solute and the free water-to-solute ratios as functions of the WSR in both bulk and single-particle measurements, shown as filled and empty symbols, respectively. Unlike NaCl or $MgSO_4$ but similar to $(NH_4)_2SO_4$, the amounts of free and solvated water in the single-particle measurements are very close in the whole concentration range for $Mg(NO_3)_2$. Nevertheless, one can see that the difference between the solvated water-to-solute ratio and the free water-to-solute ratio decreases as the WSR decreases from large values (e.g., WSR = 50). Forcing linear fits on the free and solvated water ratios yields that they are equal at a WSR of about 6.4, close to the saturation condition of bulk $Mg(NO_3)_2$ at WSR about 6.7 (ref 24). Significant contact ion pairing between magnesium and nitrate ions occurs at a WSR of about 6, as revealed by the structural changes in the Raman nitrate peak at around 1050 cm^{-1} (ref 12). The particle with a WSR of 2 at 0% RH has the stoichiometry of the $Mg^{2+}(H_2O)_2(NO_3^-)_2$ (C_{2h}) bidentate contact ion pair.

Similar to those of NaCl, Na_2SO_4, and $(NH_4)_2SO_4$, the bulk and single-particle measurements of $Mg(NO_3)_2$ droplets are not consistent. It is unlikely that the discrepancy between the bulk and single-particle data is due to optical artifacts because not all of the compounds we have studied show inconsistency between the bulk and single-particle data. In fact, the bulk and single-particle measurements are consistent for sucrose[1] and $MgSO_4$. For $Mg(NO_3)_2$, the solvated water-to-solute ratio decreases with decreasing WSR in the single-particle measurements but remains more or less constant at about 5 in the bulk measurements. This suggests that the amount of free water in the bulk solutions is greater than that in single droplets of the same concentration.

(c) Spatial Heterogeneity in Aqueous Droplets. On the basis of the fluorescence images of the droplets, Choi et al.[1] observed a distribution of the state of water within the NaCl droplets and found that the PIR (the solvated-to-free water ratio) is higher near the surface of the droplets than in the core as shown in Figure 1b. In our previous study,[1] we found that the oscillating PIR patterns at different RH have the same trends, but these oscillations are not due to Mie morphological resonances, which would produce significantly different spectra even at very small changes in particle diameter. We have also confirmed that they are not optical artifacts because the imaging spectra of sucrose droplets are independent of whether the droplets are irradiated by the laser from above or below. As mentioned in the Experimental Section, the error in PIR within a particle at a specific RH is about 10%, which indicates high reproducibility in the imaging measurements even with a lower single-to-noise ratio than the fluorescence measurements. Figure 10a and b show the PIR of Na_2SO_4 and $(NH_4)_2SO_4$ droplets at a RH of about 80% and 60%, indicated by empty and filled symbols, respectively. Overall, the PIR increases and approaches unity when the RH decreases. Similar to the PIR for NaCl, the PIR values for both Na_2SO_4 and $(NH_4)_2SO_4$ droplets are not uniform, with higher values near the edges and roughly constant values in the core. The PIR distributions suggest that there is relatively more solvated water at the surface than in the core of the droplet, although this is a relative comparison between the core and the surface. It does not mean that there is more solvated water than free water at the surface. We also note that the difference of the PIR near the surface and at the center is more drastic in the diluted droplets. Because the patterns in Figure 10a and b are similar, it is possible that this is a solvation property of sulfate ions in droplets.

By analyzing the photoemission spectra of sulfate ions, Wang et al.[25] found that most sulfate ions are located in the center of the water clusters. Recently, Jungwirth et al.[26] predicted from molecular dynamics simulations that sulfate ions prefer interior solvated over surface solvated. It is interesting to note that composition heterogeneity exists in both the angstrom-scale surface domains reported on the droplet/air interface in the literature and the micrometer-scale outer domains reported for

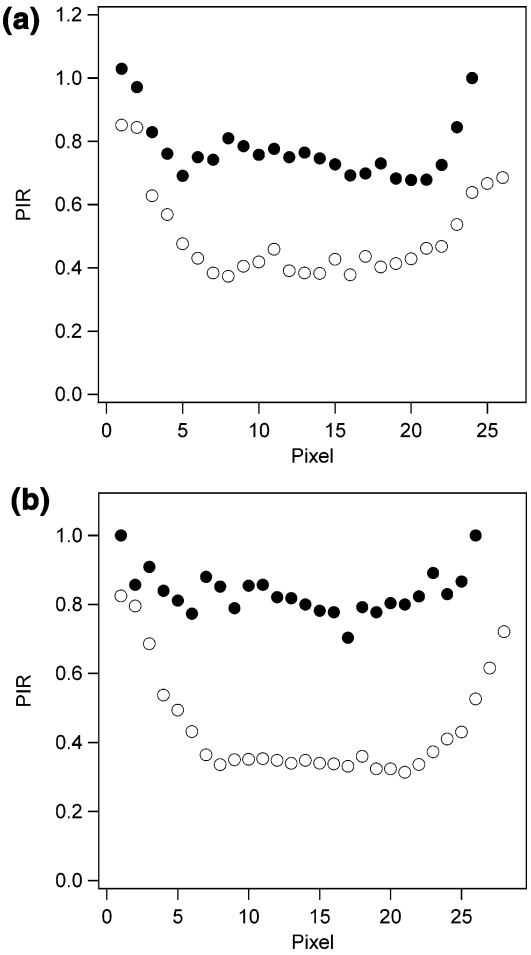

Figure 10. (a) The PIR of a sodium sulfate droplet along the vertical axis of the droplet. ○, PIR at RH = 80%; ●, PIR at RH = 60%. (b) The PIR of an ammonium sulfate droplet along the vertical axis of the droplet. ○, PIR at RH = 80%; ●, PIR at RH = 60%.

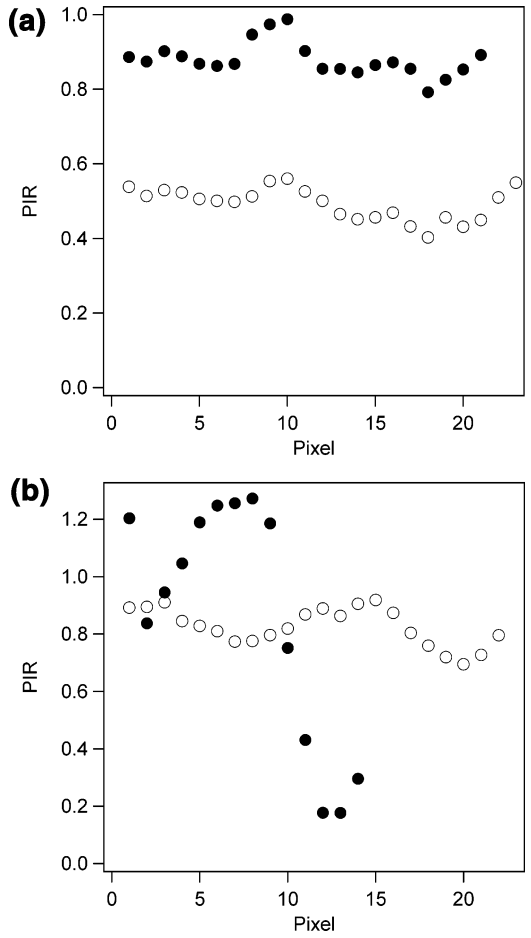

Figure 11. (a) The PIR of a magnesium sulfate droplet along the vertical axis of the droplet. ○, PIR at RH = 80% (WSR ≈ 12); ●, PIR at RH = 40% (WSR ≈ 5.2). (b) The PIR of a magnesium nitrate droplet along the vertical axis of the droplet. ○, PIR at RH = 80% (WSR ≈ 12); ●, PIR at RH = 10% (WSR ≈ 3).

supermicrometer-sized particles in this study, although the underlying principles are likely different.

Figure 11a shows the fluorescence imaging results of $MgSO_4$ droplets at WSR of 12 and 5.2 (RH about 80% and 40%). In contrast to the results for Na_2SO_4 and $(NH_4)_2SO_4$ droplets, the PIR distribution in the $MgSO_4$ droplets at different RH is quite uniform at both RH values. $MgSO_4$ does not show the structural heterogeneity that Na_2SO_4 and $(NH_4)_2SO_4$ do, probably due to the formation of contact ion pairs between the magnesium and sulfate ions, which alters the solvation property of $MgSO_4$.

Figure 11b shows the fluorescence imaging results of $Mg(NO_3)_2$ droplets in terms of the PIR as a function of location in the droplet at WSR of 12 and 3 (RH about 80% and 10%), indicated by empty and filled symbols, respectively. Pixels 1 and 22 (15 for filled symbols) represent the bottom and top edges of the droplet, respectively. The size of the droplet at low RH is much smaller than that at high RH due to evaporation of the water. The PIR oscillates significantly at low RH but is relatively uniform at high RH. Such oscillations have been reported for droplets of sucrose and glucose.[1] Although the PIR distribution at low RH is not symmetrical and the PIR of pixel 1 is high, the average PIR near the edges (top and bottom) of the droplet is lower than at the center. This indicates that there is a structural heterogeneity in the state of water in particles at low RH (ref 1).

The observation of a lower PIR near the surface of $Mg(NO_3)_2$ droplets at a WSR of 5.2 suggests that there are fewer solvated water and more nitrate ions (i.e., contact ion pairs) bound to the magnesium ions near the surface. This is consistent with our recent Raman imaging results of the solvation characteristics of $Mg(NO_3)_2$ droplets.[12] On the basis of the Raman peak characteristics of the ν_1 NO_3^- peak at about 1050 cm^{-1} from $Mg(NO_3)_2$ droplets equilibrated at different RH, Zhang et al.[12] reported that supersaturated $Mg(NO_3)_2$ droplets (WSR = 2.8) are structurally heterogeneous but diluted droplets (WSR = 9.6) are homogeneous. They proposed that these supersaturated droplets consist of a center region of predominantly monodentate and bidentate contact ion pairs with structures of $[Mg^{2+}(H_2O)_5NO_3^-]$ and $[Mg^{2+}(H_2O)_4NO_3^-]$ and an outer region of monodentates with a structure of $[Mg^{2+}(H_2O)_{6-x}(NO_3^-)_x$, x = 3,4,5,6]. This notion of a structure with more solvated water molecules and fewer bound nitrate ions near the center than in the outer region near the surface is consistent with the fluorescence results shown in Figure 11b. The outer region is more complex than the region near the center as the ratio of solvated water to free water decreases toward the surface. Nitrate enrichment near the surface of solutions has been predicted by molecular simulation.[27] However, the simulation was performed at a very low concentration of 1 nitrate ion and 555 water molecules, and it may not be related to our observations. Our Raman and fluorescence studies focus on the formation of contact ion pairs at high concentrations.

Table 1 shows the comparison between the free water and solvated water-to-solute ratios in the core region of the single particles (calculated from the imaging results) and the bulk solutions at 80% RH. We found that the results are consistent

TABLE 1: Comparison of the Ratios of Free and Solvated Water to Solute in Single-Particle Imaging Experiments and Bulk Measurements

	single particle imaging measurements				bulk measurements	
compound	free water (core)	solvated water (core)	free water (average)	solvated water (average)	free water	solvated water
Sucrose (Choi et al.[1])	3.7	4.9	3.6	5.0	3.7	4.4
NaCl (Choi et al.[1])	7.9	3.1	7.7	3.3	8.4	2.6
$(NH_4)_2SO_4$	7.1	2.4	6.8	2.7	8.8	0.7
Na_2SO_4	7.9	3.1	7.4	7.6	9.7	1.3
$MgSO_4$	8.2	3.8	8.3	3.7	8.9	3.1
$Mg(NO_3)_2$	6.8	5.8	6.9	5.7	7.7	4.9

within experimental error for sucrose and magnesium sulfate, while those for ammonium sulfate, sodium sulfate, and magnesium nitrate show significant inconsistency. This may be due to the large deviations in the state of water between the single-particle and bulk measurements of ammonium sulfate, sodium sulfate, and magnesium nitrate. This indicates that, at the same concentration, the free and solvated water distribution of these compounds in single droplets is different from that in bulk solutions. Although NaCl also shows heterogeneity in the state of water in the imaging experiments, the difference between the single-particle and bulk measurements is not as significant as that of ammonium sulfate and sodium sulfate.

By comparing the results of all of the compounds studied in this paper and those by Choi et al.,[1] we note that the compounds that show inconsistency between bulk and single-particle measurements (e.g., NaCl, $(NH_4)_2SO_4$, and Na_2SO_4) also show structural heterogeneity by fluorescence imaging, while those that have consistent bulk and single-particle measurements ($MgSO_4$) show homogeneous structures. An exception is sucrose in Choi et al.[1] and $Mg(NO_3)_2$ in this study. For the case of $Mg(NO_3)_2$, only the highly concentrated solutions are heterogeneous, but the bulk and single-particle measurements are not consistent. Spatial heterogeneity affects the surface concentration of dissolved species in an aerosol droplet and can have profound effects on the heterogeneous atmospheric chemistry of aerosols.[28]

Conclusion

Using fluorescence spectroscopy, we have made a number of observations about the behavior of aqueous aerosol droplets, including efflorescence and molecular heterogeneity, which have not been reported before. The state of water, obtained from a combination of hygroscopic and fluorescence measurements, is useful in understanding the properties of aerosol droplets. Efflorescence of supersaturated droplets is associated with the equality of free and solvated water. Fluorescence imaging results suggest that droplets can be heterogeneous in terms of their solvated-to-free water ratios. Complementing our earlier work on Raman spectroscopy and the hygroscopic properties of aerosols, the use of fluorescence spectroscopy with pyranine provides another channel through which to understand the hygroscopic properties and phase transformations of aerosols on a molecular level.

Acknowledgment. This work was supported by the Research Grants Council of the Hong Kong Special Administrative Region, China (Project No. HKUST6042/01P). We would like to thank Scot Martin for suggestions and discussions on the manuscript and another reviewer for comments.

References and Notes

(1) Choi, M. Y.; Chan, C. K.; Zhang, Y. H. *J. Phys. Chem. A* **2004**, *108*, 1133.
(2) Martin, S. T. *Chem. Rev.* **2000**, *100*, 3403.
(3) Han, J.; Martin, S. T. *J. Geophys. Res.* **1999**, *104*, 3543.
(4) Martin, S. T.; Salcedo, D.; Molina, M. J. *Geophys. Res. Lett.* **1998**, *25*, 31.
(5) Martin, S. T.; Salcedo, D.; Molina, L. T.; Molina, M. J. *J. Phys. Chem. B* **1997**, *101*, 5307.
(6) Ha, Z.; Chan, C. K. *Aerosol Sci. Technol.* **1999**, *31*, 154.
(7) Zhang, Y. H.; Chan, C. K. *J. Phys. Chem. A* **2003**, *107*, 5956.
(8) Chakraborty, R.; Berglund, K. A. *J. Cryst. Growth* **1992**, *125*, 81.
(9) Cohen, M. D.; Flagan, R. C.; Seinfeld, J. H. *J. Phys. Chem.* **1987**, *91*, 4563.
(10) Zhang, Y. H.; Chan, C. K. *J. Phys. Chem. A* **2000**, *104*, 9191.
(11) Zhang, Y. H.; Chan, C. K. *J. Phys. Chem. A* **2002**, *106*, 285.
(12) Zhang, Y. H.; Choi, M. Y.; Chan, C. K. *J. Phys. Chem. A* **2004**, *108*, 1712.
(13) Davis, E. J. *Aerosol Sci. Technol.* **1997**, *26*, 212.
(14) Pouxviel, J. C.; Dunn, B.; Zink, J. I. *J. Phys. Chem.* **1989**, *93*, 2134.
(15) Aguedo, M.; Wache, Y.; Belin, J. M. *FEMS Microbiol. Lett.* **2001**, *200*, 185.
(16) Haswgawa, M. *Langmuir* **2001**, *17*, 1426.
(17) Yedur, S. K.; Berglund, K. A. *Appl. Spectrosc.* **1996**, *50*, 866.
(18) Tang, I. N.; Fung, K. H.; Imre, D. G.; Munkelwitz, H. R. *Aerosol Sci. Technol.* **1995**, *23*, 443.
(19) Neubauer, K. R.; Johnson, M. V.; Wexler, A. S. *Atmos. Environ.* **1998**, *32*, 2521.
(20) Ohtaki, H.; Radnal, T. *Chem. Rev.* **1993**, *93*, 1157.
(21) Rudolph, W. W.; Irmer, G.; Hefter, G. T. *Phys. Chem. Chem. Phys.* **2003**, *5*, 5253.
(22) Chan, C. K.; Ha, Z.; Choi, M. Y. *Atmos. Environ.* **2000**, *34*, 4795.
(23) Choi, M. Y.; Chan, C. K. *J. Phys. Chem. A* **2002**, *106*, 4566.
(24) Robinson, R. A.; Stokes, R. H. *Electrolyte Solutions*, 2nd ed.; Butterworths: London, 1970.
(25) Wang, X. B.; Yang, X.; Nicholas, J. B.; Wang, L. S. *Science* **2001**, *294*, 1322.
(26) Jungwirth, P.; Curtis, J. E.; Tobias, D. J. *Chem. Phys. Lett.* **2003**, *367*, 704.
(27) Knipping, E. M.; Lakin, M. J.; Foster, K. L.; Jungwirth, P.; Tobias, D. J.; Gerber, R. B.; Dabdub, D.; Finlayson-Pitts, B. J. *Science* **2000**, *288*, 301.
(28) Salvador, P.; Curtis, J. E.; Tobias, D. J.; Jungwirth, P. *Phys. Chem. Chem. Phys.* **2003**, *5*, 3752.